J Neurophysiol 98: 1751–1762, 2007.
First published June 27, 2007; doi:10.1152/jn.00460.2007.

Frontoparietal Activation With Preparation for Antisaccades

Matthew R. G. Brown,[1,2,3] Tutis Vilis,[1,2] and Stefan Everling[1,2,4]

[1]*Department of Physiology and Pharmacology,* [2]*Department of Psychology, and* [3]*Graduate Program in Neuroscience, University of Western Ontario; and* [4]*The Centre for Brain and Mind, Robarts Research Institute, London, Ontario, Canada*

Submitted 24 April 2007; accepted in final form 22 June 2007

Brown MRG, Vilis T, Everling S. Frontoparietal activation with preparation for antisaccades. *J Neurophysiol* 98: 1751–1762, 2007. First published June 27, 2007; doi:10.1152/jn.00460.2007. Several current models hold that frontoparietal areas exert cognitive control by biasing task-relevant processing in other brain areas. Previous event-related functional magnetic resonance imaging (fMRI) studies have compared prosaccades and antisaccades, which require subjects to look toward or away from a flashed peripheral stimulus, respectively. These studies found greater activation for antisaccades in frontal and parietal regions at the ends of long (≥6 s) preparatory periods preceding peripheral stimulus presentation. Event-related fMRI studies using short preparatory periods (≤4 s) have not found such activation differences except in the frontal eye field. Here, we identified activation differences associated with short (1-s) preparatory periods by interleaving half trials among regular whole trials in a rapid fMRI design. On whole trials, a colored fixation dot instructed human subjects to make either a prosaccade toward or an antisaccade away from a peripheral visual stimulus. Half trials included only the instruction and not peripheral stimulus presentation or saccade generation. Nonetheless, half trials evoked stronger activation on antisaccades than on prosaccades in the frontal eye field (FEF), supplementary eye field (SEF), left dorsolateral prefrontal cortex (DLPFC), anterior cingulate cortex (ACC), intraparietal sulcus (IPS), and precuneus. Greater antisaccade response-related activation was found in FEF, SEF, IPS, and precuneus but not in DLPFC or ACC. These results demonstrate greater preparatory activation for antisaccades versus prosaccades in frontoparietal areas and suggest that prefrontal cortex and anterior cingulate cortex are more involved in presetting the saccade network for the antisaccade task than generating the actual antisaccade response.

INTRODUCTION

Primates are not constrained to react to sensory stimuli with reflexive movements, but they rather can acquire almost arbitrary stimulus-response associations. The ability to execute different responses to identical stimuli has been attributed to differences in preparatory set, i.e., the intention and readiness to perform a certain task (Evarts et al. 1984; Hebb 1972). Examples of two tasks that require very different preparatory sets are the prosaccade and antisaccade tasks (Everling and Fischer 1998; Hallett 1978; Hallett and Adams 1980). The prosaccade task requires subjects to look toward a flashed peripheral stimulus, whereas the antisaccade task requires subjects to suppress the automatic saccade to the stimulus and instead to look away from the stimulus to its mirror location in the opposite visual hemifield. To correctly perform this task, the neural process that triggers the automatic prepotent response to look toward the stimulus must be suppressed so that the vector inversion for the antisaccade can be computed and the saccade can be executed. Single-neuron recordings in nonhuman primates have demonstrated that the brain accomplishes this task by reducing the level of preparatory saccade-related activity in the superior colliculus before stimulus presentation on antisaccade trials (Munoz and Everling 2004). Neural correlates for different preparatory sets associated with prosaccades and antisaccades have been identified in several frontal cortical brain areas in nonhuman primates, including the frontal eye field (FEF) (Everling and Munoz 2000), supplementary eye field (SEF) (Amador et al. 2004), dorsolateral prefrontal cortex (DLPFC) (Everling and DeSouza 2005; Johnston and Everling 2006a,b), and anterior cingulate cortex (ACC) (Johnston et al. 2007). Single-neuron recording has also been used to compare prosaccades and antisaccades in the lateral intraparietal area (LIP) (Gottlieb and Goldberg 1999; Zhang and Barash 2000, 2004), but these studies did not investigate preparatory differences between the two tasks. Specifically, they did not compare neuronal discharge patterns between prosaccades and antisaccades during the preparatory period in which monkey subjects had been given the trial-type instruction cue but had not seen a peripheral stimulus or responded to it with an eye movement.

Studies recording event-related potentials (ERPs) in human subjects have found a higher negative potential before antisaccades than before prosaccades over a wide range of recording sites, supporting the idea that cortical areas in humans exhibit neural correlates for different preparatory sets associated with prosaccades and antisaccades (Everling et al. 1997; Klein et al. 2000). Connolly and colleagues (2002) directly compared the activation in the frontal eye field and intraparietal sulcus (IPS) between prosaccades and antisaccades by using an event-related functional magnetic resonance imaging (fMRI) paradigm. Their paradigm included a gap of 0, 2, or 4 s, during which the subject viewed a black screen, between the disappearance of the central fixation point and peripheral stimulus onset. The authors found greater preparatory activation for antisaccades compared with prosaccades in FEF but not in IPS. Based on this finding they concluded that the human FEF, but not the IPS, is critically involved in preparatory set. The absence of any parietal activation during the preparatory period for antisaccades is somewhat surprising given the activation of a frontoparietal network with many different kinds of tasks (Cabeza and Nyberg 2000; Duncan and Owen 2000).

A potential problem with the analysis carried out by Connolly and colleagues is that they shifted the time courses on which they performed their analysis by 3 s to account for

Address for reprint requests and other correspondence: S. Everling, The Centre for Brain and Mind, Robarts Research Institute, 100 Perth Drive, London, Ontario N6A 5K8, Canada (E-mail: severlin@uwo.ca).

The costs of publication of this article were defrayed in part by the payment of page charges. The article must therefore be hereby marked "*advertisement*" in accordance with 18 U.S.C. Section 1734 solely to indicate this fact.

hemodynamic lag. Therefore the generation of the saccade, itself, might have contributed to apparent preparatory differences. To avoid this problem, several studies have used event-related fMRI design with compound trials consisting of a long preparatory period (6–14 s) and a response period (Curtis and D'Esposito 2003; Desouza et al. 2003; Ford et al. 2005). Although not consistent, together these studies have reported a higher activation for antisaccades than for prosaccades in a variety of cortical areas during the preparatory period, including DLPFC, FEF, ACC, presupplementary motor area (SMA), IPS, and parieto-occipital sulcus.

A direct comparison between the results from these designs with very long preparatory periods (>6 s) and the results from electrophysiological studies in nonhuman primates and ERP studies in humans that usually have short preparatory periods (<2 s) is potentially difficult due to additional processes that might be initiated during long delays. In addition, the long intertrial intervals in these event-related fMRI studies (12 or 14 s) likely lead to fatigue and might reduce task-related preparatory activations.

In a rapid event-related fMRI comparison of saccades and countermanded saccades, Curtis et al. (2005) recently showed that catch trials, in which subjects neither saw peripheral stimuli nor made saccade responses, evoked significant frontoparietal fMRI activation. The authors attributed this activation to covert attention. It is not yet known whether catch trial-evoked activation might be modulated by task type. Here, we compared prosaccades and antisaccades using a rapid event-related fMRI design that included both whole trials and catch trials, which we will call *half trials*. Whole prosaccade and antisaccade trials included a 1-s preparatory period, in which a colored fixation point indicated the trial type, followed by a response period, in which subjects made a prosaccade toward or an antisaccade away from a flashed peripheral stimulus. Half trials included only the preparatory period (Ollinger et al. 2001a,b). Subjects did not know whether a given trial would be a whole or half trial until the peripheral stimulus appeared or failed to appear, respectively. Our results show that the preparatory activation for an antisaccade, even with no executed saccade, is greater than the preparatory activation for a prosaccade in frontoparietal regions of the human brain.

METHODS

All procedures were approved by the University Research Ethics Board for Health Sciences Research at the University of Western Ontario, London, Ontario, Canada and are in accordance with the 1964 Declaration of Helsinki.

Subjects

Eleven human subjects (nine female, two male) participated in this study after giving informed written consent. Subject age ranged from 20 to 28 yr with a mean of 25 yr. Subjects reported no history of neurological or psychiatric disorder, and they had normal or corrected-to-normal vision. Two subjects described themselves as left-handed whereas the rest described themselves as right-handed.

fMRI data acquisition procedure

All fMRI data were acquired on a whole body 4-Tesla MRI system (Varian, Palo Alto, CA; Siemens, Erlangen, Germany) operating at a slew rate of 120 $mT \cdot m^{-1} \cdot s^{-1}$. A transmit only–receive only (TORO) cylindrical hybrid birdcage radio frequency (RF) head coil (Barberi et al. 2000) was used for transmission and detection of the signal.

Imaging planes for the functional scans were defined based on a series of sagittal anatomical images acquired using T1-weighting. Eleven contiguous functional planes (5 mm thick) were prescribed axially from the top of the brain to the level of the dorsal caudate and thalamus. A constrained, three-dimensional (3D) phase-shimming procedure (Klassen and Menon 2004) was used to optimize the magnetic field homogeneity over the functional volume. During each functional task, blood oxygenation level–dependent (BOLD) images (T_2^*-weighted) were acquired continuously using an interleaved, two-segment, optimized spiral imaging protocol [volume collection time = 1.0 s, repeat time (TR) = 500 ms, echo time (TE) = 15 ms, flip angle = 30°, 64 × 64 matrix size, 22.0 × 22.0-cm field of view (FOV), 3.44 × 3.44 × 5.00-mm voxel resolution]. Each image was corrected for physiological fluctuations using navigator echo correction. A corresponding high-resolution T1-weighted structural volume was acquired during the same scanning session using a 3D spiral acquisition protocol [TE = 3.0 ms, inversion time (TI) = 1,300 ms, TR = 50 ms] with a voxel resolution of 0.9 × 0.9 × 1.25 mm. Each subject was immobilized during the experimental session within a head cradle that was packed with foam padding.

Eye tracking

Visual stimuli were presented during fMRI scanning using a Silent Vision SV-4021 projection system from Avotec (Stuart, FL). The system includes an MEyeTrack-SV (Silent Vision) eye tracker from SensoMotoric Instruments (Teltow, Germany). This setup uses fiber optics housed in dual stalks positioned over the subject's eyes to allow simultaneous presentation of visual stimuli and CCD video-based infrared eye tracking. The visual display subtends 30° horizontally by 23° vertically with a resolution of 800 × 600 pixels and a refresh rate of 60 Hz. Eye tracking was also performed at a 60-Hz sampling rate with an accuracy of approximately 1°. Before scanning, we calibrated the system with a nine-point calibration, with four points in the corners, four points at the midpoints of the sides, and one point in the center of the visual display. All experimental targets were within the range of the calibration. Analysis of the eye movement signals was performed off-line.

Experimental design

This experiment compared the prosaccade and antisaccade tasks in a rapid event-related fMRI design (Fig. 1). Two thirds of prosaccade and antisaccade trials were whole trials, whereas the remaining third consisted of half trials. When not performing a task response, the subject fixated a central white dot (0.6° diameter). An individual trial started when the central dot changed from white to magenta or cyan, where color indicated whether the current trial was a prosaccade or antisaccade trial. For six of the subjects, cyan and magenta mapped, respectively, onto the antisaccade and prosaccade tasks, whereas for the other five subjects, the mapping was reversed. The colored fixation point was presented for 1 s, followed by a 200-ms gap, during which the subject was presented with a black screen. The 200-ms gap was included because it is known to decrease the fixation-related activity and increase the saccade-related activity in the superior colliculus (Dorris et al. 1997; Everling et al. 1999), resulting in a larger proportion of erroneous prosaccade responses on antisaccade trials (Bell et al. 2000; Fischer and Weber 1992, 1997; Forbes and Klein 1996) and an increased demand for cognitive control before stimulus onset (Munoz and Everling 2004). On whole trials, a peripheral stimulus (0.6° diameter white dot) was presented at the end of the 200-ms gap. The peripheral stimulus could appear to the left or right of fixation, at eccentricities of 6 or 10°, either on the horizontal meridian or 20° clockwise or counterclockwise relative it. The pe-

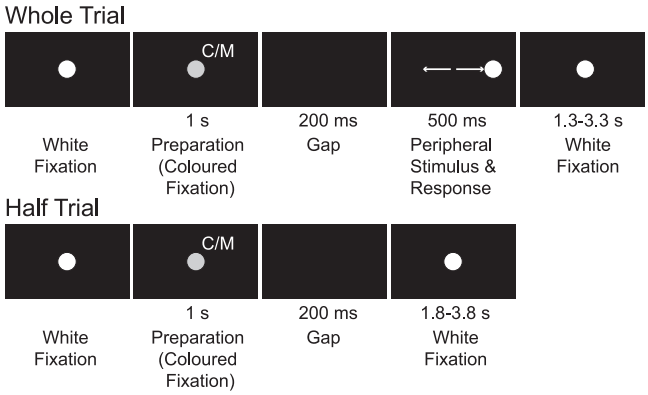

FIG. 1. Schematic respresentation of timing and visual stimulus presentation for prosaccade and antisaccade whole and half trials. Gray fixation point and "C/M" in the preparation panel (2nd from *left*) denote that the white fixation point changed to magenta or cyan to instruct the subject whether to make a prosaccade or antisaccade on stimulus presentation. Color-trial-type assignment depended on the subject. Small white arrows in the 4th panel for the whole trial indicate a rightward prosaccade response and a leftward antisaccade response. Whereas whole trials contained both the preparation and response events, half trials contained only the trial-type preparation. On half trials, subjects never saw a peripheral stimulus nor made an eye movement. Half trials allowed us to measure preparatory activation separately from response-related activation. See METHODS for details.

ripheral stimulus was presented for 500 ms, after which it disappeared simultaneously with the reappearance of the central white fixation dot. Before the peripheral stimulus disappeared, the subject had to look at it on prosaccade trials or look away from it, toward its mirror location in the opposite visual quadrant, on antisaccade trials. The subject then had to return gaze to center and maintain central fixation on the newly reappeared central white fixation dot. On half trials, the central fixation dot reappeared at the end of the 200-ms gap; no peripheral stimulus was presented and the subject was required simply to maintain central fixation without generating either a prosaccade or antisaccade response. Half trials provided a measure of preparatory activation patterns separate from response-related signals. The subject did not know whether a given trial would be a whole or half trial until the peripheral stimulus appeared or failed to appear, respectively. The time interval between the starts of adjacent trials was 3, 4, or 5 s, randomized with a mean of 4 s (uniform distribution). This jittering was done to decorrelate the fMRI signal components evoked by individual trial types allowing for deconvolution as subsequently described (Dale 1999).

Each subject performed eight to 15 data collection runs (median 12 runs; total 122 runs across all 11 subjects). An individual run lasted 316 s. One run consisted of 73 trials (24 whole prosaccade trials, 12 half prosaccade trials, 24 whole antisaccade trials, 12 half antisaccade trials, and the first trial of the run). The first trial of a run, which was a whole prosaccade trial on half of the runs and a whole antisaccade trial on the other half, was modeled separately because it could not be counterbalanced in terms of the preceding trial type, given that there was no preceding trial. Each of the 12 possible peripheral stimulus locations (see above) was used twice for the whole prosaccade and whole antisaccade trials in a given run. In addition, the first trial of the run always used a peripheral stimulus with 6° eccentricity and 20° clockwise relative to the horizontal meridian on the right side. The order and timing structure of the trial presentation sequence within each run were determined using computerized random search to minimize correlation among different trial types and to ensure first-order counterbalancing of trial parameters (prosaccade vs. antisaccade, half vs. whole trials, left vs. right peripheral stimulus) in the forward and backward directions.

We chose to present whole and half trials at a 2:1 ratio (see above) based on a compromise between two criteria. We presented half trials less frequently than whole trials so that subjects would not come to expect a large proportion of trials to be half trials with no response requirement. This expectation might have attenuated the recruitment of preparatory processes evoked by the instruction cue. On the other hand, we had to include enough half trials to allow for decent statistical precision when deconvolving half-trial activation profiles (see *Statistical analysis and linear deconvolution* below for details of deconvolution). We decided that a 2:1 ratio of whole to half trials was a good compromise between these two competing concerns, and pilot studies confirmed this.

On the day of an experiment, subjects were instructed on task performance and given 5–15 min of practice until they were comfortable with the tasks. Within 15 min, all subjects were able to perform the tasks competently as assessed by the authors' visual inspection. We also recorded subject behavior to verify performance, as described in the next section.

Behavioral analysis

We used video eye tracking data collected concurrently with fMRI scanning to determine saccadic response latencies and saccade endpoints. We discarded trials with several types of mistakes including prosaccade and antisaccade error trials, failure to respond, excessively short or long response latency (latency $<$100 ms or latency $>$500 ms, respectively), and failure to maintain fixation. The average proportion of trials discarded for any of these reasons was 10.6 $\pm$ 5.2% (SD) with a range of 3.2 to 19.1%, across all 11 subjects. Prosaccade error trials, in which subjects incorrectly made antisaccade rather than prosaccade responses, constituted 2.8 $\pm$ 2.1% of prosaccade whole trials on average. Error antisaccade trials, in which subjects failed to inhibit the automatic saccade and generated prosaccade responses, constituted 14.7 $\pm$ 8.9% of antisaccade whole trials on average. We did not analyze error trials because half trials, which contained no response events, could not be classified in terms of correct and error performance, preventing us from measuring preparatory activation separately from response-related activation on error trials. Percentages of trials discarded due to failure to maintain fixation during fixation periods were as follows: prosaccade half trials 0.9 $\pm$ 0.9% (mean and SD), antisaccade half trials 1.9 $\pm$ 2.5%, prosaccade whole trials 0.4 $\pm$ 0.4%, and antisaccade whole trials 0.7 $\pm$ 0.9%.

Preprocessing

Preprocessing was done using Matlab 6 (The MathWorks, Natick, MA) and BrainVoyager 2000 (Brain Innovation, Maastricht, The Netherlands). We removed the first four volumes from each voxel's time course to allow for complete spin saturation. We performed nonlinear trend removal on the data using a running lines smoother programmed in Matlab 6. This algorithm corrected time courses for low-frequency trends, as described in APPENDIX A of Brown et al. (2006), and has the advantage of being robust against edge effects. The trend removal algorithm also removed spikes in the signal, defined as any point greater than 3SDs from the mean, trend-removed signal. All functional data were superimposed onto 3D anatomical images, resampled into 3 $\times$ 3 $\times$ 3-mm^3 voxels, aligned onto the anterior commissure–posterior commissure axis, and scaled to Talairach space with BrainVoyager 2000. Functional data underwent 3D motion correction by trilinear interpolation of each volume to a single reference functional volume. Mean subject head translation was 0.07 $\pm$ 0.04 mm (SD) and mean subject head rotation was 0.13 $\pm$ 0.06°. Maximum motion across all subjects was 0.14-mm translation and 0.25° rotation. We did not exclude any subjects on the basis of motion. Functional data were smoothed with a spatial low-pass filter using a low-pass cutoff of 0.063 cycle/mm in the Fourier domain. Finally, voxel time courses were scaled into percentage signal change

values on a run-by-run basis using the mean time course across the run as baseline.

Statistical analysis and linear deconvolution

Because we used a rapid event-related design, with trial onset spacing randomized from 3 to 5 s with a mean of 4 s (uniform distribution), the BOLD signal we recorded from any given point was the sum of the BOLD impulse responses from several preceding task events. This necessitated the use of deconvolution methods to extract BOLD responses from individual task components. We used linear regression based on the general linear model (GLM) to perform both the statistical analysis and the linear deconvolution. The process of fitting a GLM to rapid event-related fMRI data can effect a linear deconvolution because it finds the best scaling of predictor curves that model overlapping, summated BOLD signal components.

We used a mixed-effects analysis based on Worsley et al. (2002). A GLM was fit to each subject's data after prewhitening to correct for colored noise covariance. Prewhitening avoids the inflation of type I error that occurs with GLM statistical tests that fail to account for colored noise in the data (Bullmore et al. 2001). Our GLM design matrix incorporated sets of finite impulse response predictor functions (Serences 2004) for eight groups of trials including *1*) correct half prosaccade trials; *2*) correct whole prosaccade trials; *3*) correct half antisaccade trials; *4*) correct whole antisaccade trials; *5*) error whole antisaccade trials (when subjects made prosaccades rather than antisaccades); *6*) the first trials of each run, which were modeled separately because they could not be counterbalanced for the preceding trial type; *7*) any prosaccade or antisaccade trials with responses >500 ms in latency; and *8*) other discarded trials with latencies within the 100- to 500-ms range. That is, for each of these groups of trials, a set of 12 impulse responses (one impulse per 1-s volume) was locked to the start of each trial in the group. Together, the 12 impulse predictors for a given group of trials, such as antisaccade whole trials, modeled the activation time course for that group of trials with one point per second over 12 s. Viewed another way, for each of the eight groups of trials, a subject's GLM design matrix contained 12 columns, with ones at the appropriate locations, to model the 12 impulse functions for that trial group (Serences 2004). The design matrix thus contained a total of 97 columns (8 groups of trials $\times$ 12 columns per trial group, plus one column for the offset predictor). The constant, offset predictor, which was composed of all ones, was included to model the baseline across all (percentage scaled) functional runs in a given subject. We chose the finite impulse response model because it makes no assumptions about the shape of the hemodynamic response function other than its length (12 s in this case). Note that this is unlike more constrained approaches, such as incorporating a gamma function into the model, which assumes that the hemodynamic response is gamma-shaped. The use of linear regression also assumes of course that the hemodynamic response is linear (Boynton et al. 1996). It was necessary to model discarded trials explicitly in the design matrix because the fMRI signals they evoked would otherwise contaminate the deconvolution of signals from adjacent correct trials. The prosaccade and antisaccade whole trials each consisted of a preparation and a response event, whereas the prosaccade and antisaccade half trials contained only the preparation event. Therefore half trials provided a measure of preparation-related fMRI activation, which was subtracted from whole trial activation patterns to yield estimates of purely response-related fMRI signals.

For each of the 11 subjects, we computed two statistical parametric maps by contrasting four pairs of activation profiles. The first contrast was antisaccade preparatory activation minus prosaccade preparatory activation over a time interval from 4 to 6 s after the instruction onset. This interval was chosen a priori because it straddles the peak of the hemodynamic impulse response curve as described previously (Boynton et al. 1996). The second contrast was antisaccade response activation minus prosaccade response activation over the time interval from 5 to 7 s after instruction onset. The response contrast time interval was shifted 1 s later than the preparation contrast interval because the onset of the peripheral stimulus which evoked a prosaccade or antisaccade response in the whole trials occurred 1.2 s after the instruction stimulus onset.

For each of the statistical contrasts, individual subject maps were combined using a mixed-effects analysis (Worsley et al. 2002), which addressed variability both within subjects and between subjects. Mixed-effects contrast maps were thresholded at a T-value of 2.0 ($P < 0.05$, uncorrected, df = 15,000) and then cluster size thresholded at a minimum size of 1,742 mm^3 to correct for multiple comparisons across the voxel population at $P < 0.05$, based on Gaussian random field theory (Worsley et al. 2002). For details of the mixed-effects analysis, see APPENDIX B of Brown et al. (2006) and Worsley et al. (2002).

Presentation of statistical analysis

We present the results of the above-described analysis in three formats. Figure 2 shows statistical parametric maps overlaid on brain slices in the typical style of the fMRI literature. The preparation and response contrast maps, computed as described earlier, are shown on

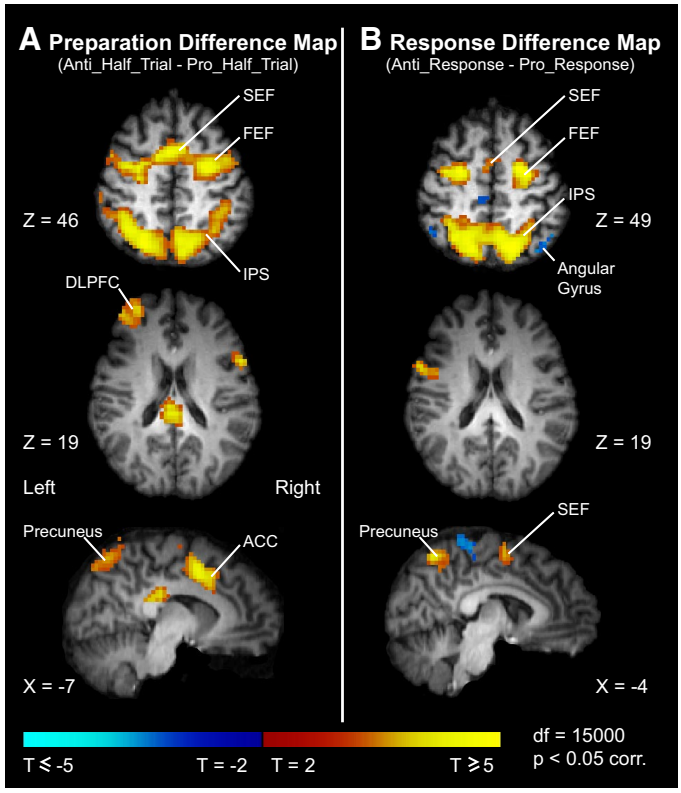

FIG. 2. Preparation and response contrast maps. *A*: preparation difference map built by contrasting antisaccade half trials with prosaccade half trials. Yellow/red regions exhibited greater antisaccade activation. Note that preparatory activation was greater for antisaccades in cortical saccade regions including the frontal eye field (FEF), supplementary eye field (SEF), and intraparietal sulcus (IPS) as well as in left dorsolateral prefrontal cortex (DLPFC), anterior cingulate cortex (ACC), and precuneus. Maps are mixed-effects maps across 11 subjects. Images obey neurological convention. *B*: response difference map built by contrasting antisaccade and prosaccade response-related activation. Response activation for both trial types was computed by subtracting half-trial activation from whole-trial activation (see METHODS and Fig. 1). Conventions as in *A*. Note that response-related activation was greater for antisaccades in FEF, SEF, IPS, and precuneus but not in left DLPFC or ACC. Response activation was greater for prosaccades in angular gyrus, which is shown in blue.

the left and right of Fig. 2, *A* and *B*, respectively. Orange and yellow voxels exhibited greater activation on antisaccades, whereas blue voxels exhibited greater activation on prosaccades. Axial slices are in neurological coordinates, with the left side of the image corresponding to the left side of the brain.

Figure 3 displays activation time courses for select regions of interest. These time courses were computed as follows. First, consider the time course one might extract from a single voxel in a single subject. In our GLM, we used sets of finite impulse response predictors for various groups of trials, as described earlier. The beta weights computed by the GLM for a specific set of finite impulse responses in fact constitute a time course for the corresponding group of trials (Serences 2004). For example, the first 12 columns of our GLM design matrix included impulses modeling the prosaccade half trials, so the first 12 beta weights in the beta weight vector computed for a given voxel would constitute that voxel's activation time course for prosaccade half trials, with one activation data point per second over 12 s. In this way, one could derive voxel-specific time courses for prosaccade and antisaccade half and whole trials. Note that in this case no special baseline adjustment would have occurred beyond the very simple baseline that is part of the GLM design matrix. By this, we refer to the last column of a subject's design matrix, which was all ones and modeled the mean activation across that subject's functional runs. Recall that all functional runs were percentage scaled during preprocessing, avoiding the necessity to model each run with its own constant offset column in the design matrix. Figure 3 shows averaged time courses and averaging was performed as follows. Time courses for each voxel in a region of interest were first derived from the beta weights on a subject-by-subject basis. For each time point in the time course, activation data were then averaged across all voxels in the region of interest and across all subjects. Regions of interest were defined from clusters of voxels exhibiting significance in either or both of the preparation or response contrasts. In right frontal eye field (FEF), supplementary eye field (SEF), right rostral intraparietal sulcus (IPS), right caudal IPS, and precuneus, we found clusters of statistically significant voxels that overlapped in both the preparation and response contrasts. The time courses for these regions were computed across the intersection of significant voxels from both contrasts. In anterior cingulate cortex (ACC) and left dorsolateral prefrontal cortex (DLPFC), we found significant voxel clusters only in the preparation contrast, and time courses for these regions were computed from the preparation contrast-derived clusters.

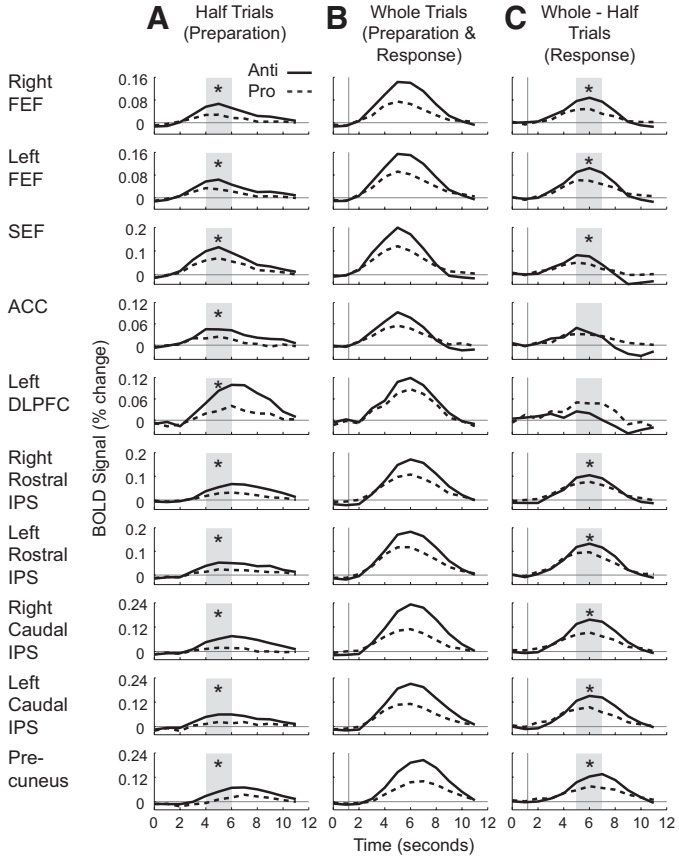

FIG. 3. Deconvolved time courses for (*A*) half trials (preparation), (*B*) whole trials (preparation and response), and (*C*) whole trials minus half trials (response). Antisaccade and prosaccade time courses are depicted with solid and dashed lines, respectively. Time courses for left and right FEF, SEF, left and right rostral IPS, left and right caudal IPS, and precuneus were derived from voxels exhibiting significance in both the preparation and response contrast maps (see Fig. 2, *A* and *B*). ACC and left DLPFC time courses were taken from voxels exhibiting significance in the preparation contrast map only because these regions showed no significant differences in the response contrast map. Gray rectangles in the *left* and *right columns* denote the 4- to 6- and the 5- to 7-s intervals used, respectively, to build the preparation and response contrast maps in Fig. 2, *A* and *B* (see METHODS). Asterisks denote statistically significant differences between antisaccades and prosaccades during the appropriate time intervals ($P < 0.05$, corrected). In *B* and *C*, the vertical gray lines positioned at 1.2 s denote the peripheral stimulus onset in whole trials. Time courses shown here were computed first by deconvolving time courses for individual voxels (see METHODS) and then averaging across voxels in a given region of interest. Ordinate units [blood oxygenated level–dependent (BOLD) percentage signal change] were derived by percentage scaling individual functional runs on a voxel-by-voxel basis using each voxel's mean activation level as baseline. Further details of deconvolution and derivation of time courses are given in the *Presentation of statistical analysis* subsection of METHODS.

Figure 4 shows the activation difference values computed in the course of building the preparation and response contrast maps. More specifically, in building the preparation and response contrast maps, we computed preparation- and response-related activation difference values (antisaccade − prosaccade) for each voxel. Recall that preparation-related activation was obtained from half trials, whereas response-related activation was obtained by subtracting half trial from whole trial activation. As described earlier, time windows of 4–6 and 5–7 s were used, respectively, for the preparation and response contrasts. These voxel-specific activation difference values were combined across subjects using the expectation maximization algorithm rather than averaging, again as described earlier. The expectation maximization algorithm also computed between-subjects variance for each difference value, and we then combined within- and between-subjects variances to derive the total variance for each voxel-specific difference value, in both the preparation and response contrasts. To derive the bar graphs shown in Fig. 4, activation difference values were averaged across all voxels in a given region of interest, where regions of interest were defined as statistically significant clusters of voxels in either the preparation or response contrast. Error bars shown in Fig. 4 were derived by averaging across voxel-specific SDs within a region of interest. Figure 4 shows activation difference values computed from the preparation contrast (*A*) and the response contrast (*B*) for all regions of interest found to be significant from both contrasts. Asterisks indicate that the activation differences are significantly greater or less than zero ($P < 0.05$, corrected for multiple comparisons) and absence of an asterisk denotes lack of significance. If a given anatomical location, such as right frontal eye field (FEF), contained statistically significant voxel clusters in both the preparation and response contrasts, then the corresponding preparation- and response-related activation difference values shown in Fig. 4, *A* and *B* were computed based on the clusters of voxels derived separately from the preparation and response contrasts. If an anatomical location exhibited a significant cluster of voxels in only one contrast, that single cluster of voxels was used to compute the activation difference values for both Fig. 4*A* and Fig. 4*B*. For example, we found a significant voxel cluster in anterior cingulate cortex (ACC) in the preparation contrast but not in the response contrast. We took this single cluster of voxels and computed the average preparation-related

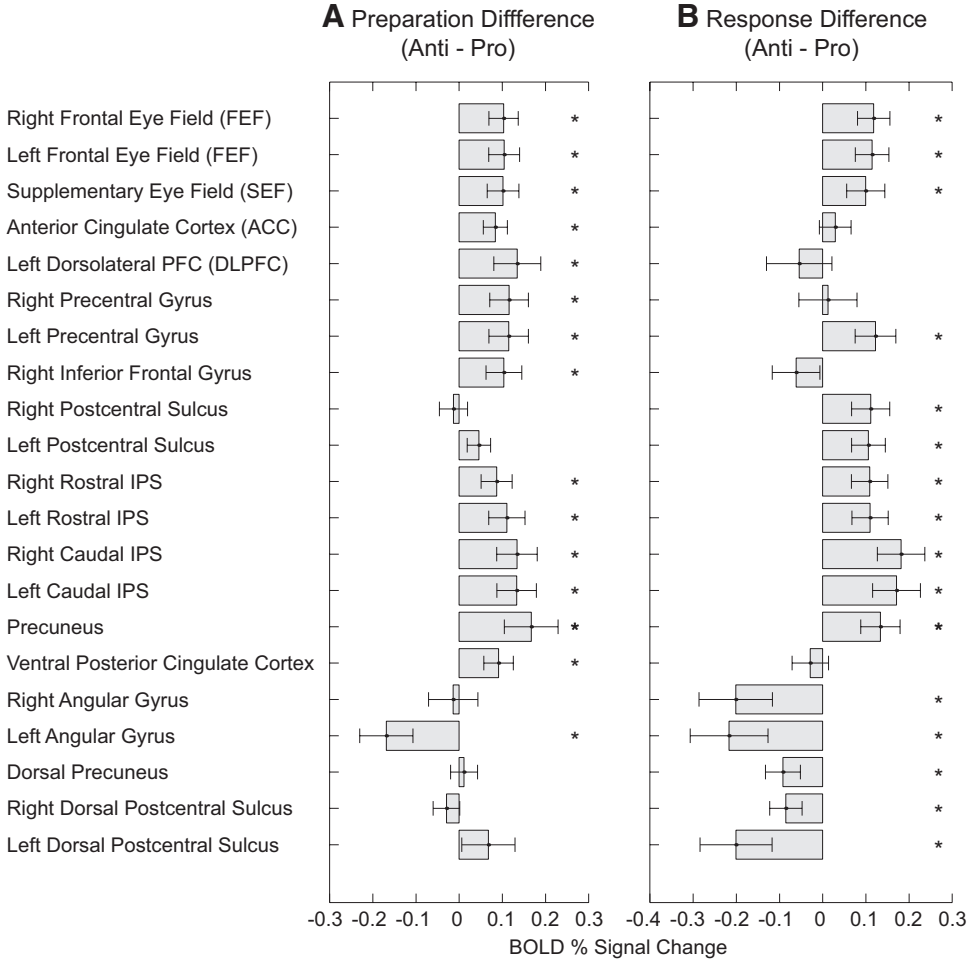

FIG. 4. Bar graphs showing mean (*A*) preparation- and (*B*) response-related activation differences (antisaccade − prosaccade) used to compute the preparation and response contrasts, respectively, that are displayed in Fig. 2. Differences are shown for all statistically significant regions in the preparation and response contrasts. Error bars are (mean) SDs of mean differences. Activation differences were computed over the 4- to 6-s time interval for preparation differences (*A*) and the 5- to 7-s interval for response differences (*B*). These time windows are also shown in Fig. 3 as light gray rectangles. Asterisks denote statistical significance ($P < 0.05$, corrected for multiple comparisons), whereas lack of an asterisk denotes lack of significance. For further details of bar graph computation, see the *Presentation of statistical analysis* subsection of METHODS. For further details of preparation and response contrasts, see *Statistical analysis and linear deconvolution* in METHODS.

activation difference across the cluster (shown in Fig. 4*A*) and we computed the average response-related activation difference across the same cluster (shown in Fig. 4*B*).

Table 1, lists direction of contrast, Talairach coordinates for statistical center of mass, and volume in cubic millimeters for all regions of interest exhibiting statistical significance in the preparation contrast (A) and the response contrast (B). Direction of contrast, denoted "Dir" in Table 1, is given as "+" to indicate greater activation on antisaccades versus prosaccades or "−" for the converse. The three Talairach coordinates for the statistical centers of mass are given in the X, Y, and Z columns. The X coordinate for the statistical center of mass (x_{CM}) of a region of interest was calculated with the following formula

$$x_{CM} = \frac{\sum_x x \sum_y \sum_z T(x, y, z)}{\sum_x \sum_y \sum_z T(x, y, z)}$$

where $T(x, y, z)$ denotes the T-statistic at a given position and x, y, and z are taken across all voxels within the region of interest. The Y and Z coordinates for the center of mass were calculated with equivalent formulae.

RESULTS

Behavior

Unlike widely spaced fMRI studies, our rapid fMRI trial design used a similar timing regimen to psychophysical and electrophysiological experiments, facilitating comparison of our results with those from these other techniques. However, despite the similarities in timing, it is still possible that the fMRI scanning environment might have altered subject performance characteristics in some way. To confirm that subject performance was similar to what has been seen in psychophysical and electrophysiological settings, we took video eye position recordings during fMRI data acquisition. We also used these recordings to exclude the few trials that contained one of several types of mistakes (see *Behavioral analysis* in METHODS). Across all 11 subjects, mean correct performance values were high, 97.2 ± 2.1% (SD) and 85.3 ± 8.9% for prosaccade and antisaccade trials, respectively. Antisaccade correct performance rates were significantly below those of the prosaccade task ($P < 0.001$, $T = 5.1$, $df = 10$), which is consistent with previous antisaccade studies (Everling and Fischer 1998). Mean saccadic latencies over all subjects were 260 ± 28 ms for correct prosaccade trials, 355 ± 36 ms for correct antisaccade trials, and 276 ± 40 ms for error antisaccade trials. Differences among these values were significant [$P < 10^{-6}$, $F(2,30) = 23.04$, one-way ANOVA]. Correct antisaccade latencies were significantly greater than correct prosaccade latencies ($P < 10^{-5}$, $T = 8.8$, $df = 10$) and significantly greater than error antisaccades latencies ($P < 10^{-5}$, $T = 8.5$, $df = 10$). Correct prosaccade latencies were significantly shorter than error antisaccade latencies ($P < 0.05$, $T = 2.4$, $df = 10$). In summary, the antisaccades in this study closely match those of other antisaccade studies, which typically find longer latencies for antisaccades compared with prosaccades and longer latencies

TABLE 1. *Preparation and response contrasts*

Region	A. Preparation Contrast					B. Response Contrast				
	Dir	X	Y	Z	Volume	Dir	X	Y	Z	Volume
Right frontal eye field (FEF)	+	27	−5	53	14,759	+	23	−8	54	7,830
Left FEF	+	28	−6	54	11,529	+	26	−8	52	8,262
Supplementary eye field (SEF)	+	0	2	50	6,048	+	0	−1	55	1,917
Anterior cingulate cortex (ACC)	+	−1	9	39	6,453					
Left dorsolateral prefrontal cortex (DLPFC)	+	32	49	21	4,212					
Right precentral gyrus	+	49	5	35	3,213					
Left precentral gyrus	+	52	4	37	1,296	+	50	4	25	2,754
Right inferior frontal gyrus	+	46	21	26	3,429					
Right postcentral sulcus						+	52	24	34	2,619
Left postcentral sulcus						+	36	33	35	2,079
Right rostral intraparietal sulcus (IPS)	+	35	47	46	6,075	+	30	48	49	2,160
Left rostral IPS	+	37	47	47	8,370	+	29	47	48	5,103
Right caudal IPS	+	16	67	48	9,342	+	17	65	51	6,669
Left caudal IPS	+	20	66	49	9,369	+	19	63	49	8,478
Precuneus	+	2	60	54	6,669	+	0	56	51	6,318
Ventral posterior cingulate cortex	+	0	27	23	2,943					
Right angular gyrus						−	44	63	40	4,347
Left angular gyrus	−	47	65	32	4,023	−	46	65	40	1,998
Dorsal precuneus						−	−5	32	60	1,836
Right dorsal postcentral sulcus						−	15	36	68	243
Left dorsal postcentral sulcus						−	32	30	65	1,323

Region of interest data for preparation contrast (A) and response contrast (B) maps. "Dir" denotes direction of contrast: greater activation for antisaccades (+) or for prosaccades (−). X, Y, and Z are the Talairach coordinates of the statistical centers of mass in millimeters. Volume is in cubic millimeters. Regions not explicitly listed as "left" or "right" straddled the midline and included voxels in both hemispheres. See *Presentation of statistical analysis* subsection in METHODS for details.

for correct compared with error antisaccades (Everling and Fischer 1998).

Preparatory activation

We compared prosaccades and antisaccades using rapid event-related fMRI to test whether a rapid fMRI design can resolve the preparatory activation differences previously observed between prosaccades and antisaccades that used widely spaced event-related fMRI. Our design included prosaccade and antisaccade half trials, consisting of only the preparation event, as a means of separating preparatory and response-related activation (see *Experimental design* in METHODS). To investigate preparatory differences between the two tasks, we built a statistical difference map by contrasting activation from antisaccade half trials with that from prosaccade half trials over a time interval from 4 to 6 s. Figure 2*A* displays the most relevant slices of this map and Table 1*A* lists the positions and sizes of regions exhibiting significant differences in the map. Figure 3 includes activation time courses for select regions. Figure 4*A* shows mean preparatory differences for all regions.

We found that cortical saccade regions typically associated with antisaccade task performance exhibited greater antisaccade versus prosaccade activation in the preparatory period. These regions included left and right frontal eye fields (FEF), bilateral supplementary eye field (SEF), left dorsolateral prefrontal cortex (DLPFC) in the left middle frontal gyrus, bilateral anterior cingulate cortex (ACC), left and right intraparietal sulcus (IPS), which contained statistically significant clusters both in the rostral and caudal portions, bilateral posterior cingulate cortex, and bilateral precuneus. In addition, the statistically "activated" voxel clusters constituting left and right FEF were continuous with activated clusters located ventrolaterally to FEF in the precentral gyrus and with a cluster in the inferior frontal gyrus on the right side. One region, DLPFC, exhibited strong hemispheric asymmetry with a large cluster of voxels (4,212 mm^3) in left DLPFC displaying greater preparatory activation for antisaccades. In right DLPFC, a much smaller cluster (837 mm^3) also displayed greater preparatory signal for antisaccades, but this cluster's size was well below the 1,742-mm^3 threshold for significance (see *Statistical analysis and linear deconvolution* subsection of METHODS).

Greater antisaccade preparatory activation is also evident in the activation time courses for the prosaccade and antisaccade half trials displayed for selected regions in Fig. 3*A*. Note that these preparatory differences manifested as soon as the hemodynamic lag would allow, with the antisaccade and prosaccade half trial activation curves separating at the 3-s mark.

We also found voxel clusters exhibiting significantly greater prosaccade preparatory versus antisaccade preparatory activation in left angular gyrus (Table 1A).

Response-related activation

The whole prosaccade and antisaccade trials contained both a preparation and a response event. To isolate response-related activation, we subtracted deconvolved time courses for the half trials, which contained only the preparation and not the response event, from the whole trial time courses. Figure 3 shows examples of activation time courses for half trials (*A*), whole trials (*B*), and the response-related activation curves generated by subtracting half trials from whole trials (*C*). Figure 4*B* shows mean response-related differences for all regions.

We contrasted antisaccade versus prosaccade response-related activation over a time interval from 5 to 7 s. The response contrast's statistical window was 1 s later than the preparation contrast's because the peripheral stimulus onset that evoked prosaccade or antisaccade responses in the whole trials oc-

curred 1.2 s after the instruction onset (see *Experimental design* and *Statistical analysis and linear deconvolution* in METHODS). Slices of the statistical map built from the response contrast are shown in Fig. 2*B* and the sizes and locations of the statistical centers of mass for significant regions are listed in Table 1B.

Many of the areas that exhibited significant differences in the preparation contrast described earlier also exhibited significant differences in the response contrast. We found voxel clusters with greater antisaccade versus prosaccade response-related activation in left and right FEF, bilateral SEF, left and right rostral IPS, left and right caudal IPS, and bilateral precuneus. There were also voxel clusters with greater antisaccade response-related activation in left precentral gyrus and left and right postcentral sulcus. Figure 3*C* shows response-related activation profiles with greater activation for antisaccade responses in left and right FEF, SEF, and left and right rostral and caudal IPS. Left DLPFC and ACC, which are also shown in Fig. 3*C*, did not display response-related differences. It is unlikely that this result was due to insufficient statistical sensitivity. Of all the voxels in the left DLPFC cluster that was significant in the preparation contrast (see above), none was individually significant in the response contrast ($P > 0.05$, without correction for multiple comparisons). Furthermore, 98% of left DLPFC voxels were not significant at $P > 0.1$ ($|T| < 1.645$, df = 15,000) and 93% were not significant at $P > 0.2$ ($|T| < 1.2815$, df = 15,000). Similarly, for voxels in the ACC cluster that exhibited significance in the preparation contrast, 92% were not significant at $P > 0.1$ ($|T| < 1.645$, df = 15,000) and 74% were not significant at $P > 0.2$ ($|T| < 1.2815$, df = 15,000). Only 2% of ACC voxels were individually significant in the response contrast ($P < 0.05$, $T > 1.96$, df = 15,000, uncorrected).

Voxel clusters with greater prosaccade compared with antisaccade response-related activation (blue regions in Fig. 2*B*) were located in left and right angular gyrus, bilateral dorsal precuneus, and left and right dorsal postcentral sulcus.

As can be seen in Fig. 3, particularly in Fig. 3*B*, BOLD time courses tended to peak at 5 s in FEF, SEF, and ACC, whereas they peaked at 6 s in left DLPFC and IPS and at 7 s in precuneus. These differences might reflect timing differences with respect to neurocomputational processing in the various regions, but it is also possible that the differences in time to peak might reflect vascular differences among the regions. For this reason, we hesitate to draw conclusions on brain function from these timing differences.

DISCUSSION

Our results show strong frontoparietal activation associated with the preparation for an antisaccade. This finding is in line with single-unit recording studies in nonhuman primates and event-related potential and event-related fMRI studies in human subjects. The data support the influential model that frontoparietal regions serve as an important source for cognitive control by biasing task-relevant processes in other brain regions (Desimone and Duncan 1995; Miller and Cohen 2001). We found that even a brief preparatory period of 1 s with no stimulus presentation and no executed saccade was sufficient to elicit a stronger BOLD fMRI activation on antisaccade trials than on prosaccade trials in frontal eye field (FEF), supplementary eye field (SEF), anterior cingulate cortex (ACC), dorsolateral prefrontal cortex (DLPFC), and intraparietal sulcus (IPS). By subtracting preparatory activation as measured in the half trials from the combination of preparation- and response-related activation measured in the whole trials, we were able to resolve response-related activation profiles. Although FEF, SEF, and IPS were also more active for the antisaccade response than the prosaccade response, the ACC and DLPFC were more active for antisaccade than prosaccade trials only during the preparatory period.

Preparatory activation

To our knowledge, this is the first fMRI study that found significantly higher preparatory activations in frontoparietal regions for antisaccades compared with prosaccades for very short preparatory periods. Our results extend those of Curtis et al. (2005) who demonstrated that short catch trials, in which subjects fixated a central fixation point and expected a peripheral stimulus to appear, evoked significant activation in frontoparietal regions. Here we have shown that this frontoparietal activation in specially designed catch trials—that is, the half trials we used in this experiment—is task dependent. Recently, we compared prosaccade, antisaccade, and nogo trials using a rapid event-related compound fMRI design and did not find differences during the preparatory period between these tasks (Brown et al. 2006). In that study, the preparation interval length was jittered to decorrelate preparation- and response-related fMRI signal components. One potential limitation of the previous study's design was that the instruction for a given trial type was always followed by the response for that trial type, introducing a sequence bias. This sequence effect might have caused any preparatory differences to be obscured by the subsequent response-related signals, which did exhibit robust differences between prosaccades and antisaccades in frontoparietal regions. We therefore suggest that a half-trial design is better suited to detect task-dependent preparatory processes than jittered compound trials in rapid fMRI.

Several previous event-related fMRI studies have found higher activations in some of these frontoparietal areas for antisaccades compared with prosaccades (Connolly et al. 2002; Curtis and D'Esposito 2003; Desouza et al. 2003; Ford et al. 2005). Connolly and colleagues found an increased activation for antisaccades compared with prosaccades in FEF but not in IPS. The authors imaged only one brain slice, and they used compound trials with very short preparatory periods (0, 2, and 4 s). Because of the hemodynamic lag, they compared levels of preparatory activation 3 s after instruction onset, and therefore response processes might have influenced this activation. The study by Curtis and D'Esposito (2003) found differences only at the end of a 7-s preparatory period in the pre-SMA. Subjects in that study were required to hold the task instruction in working memory, a process known to activate frontoparietal regions. Such a working memory–related activation in both tasks might have masked any further potential differences between the preparation of prosaccades and antisaccades. As in the present study, Ford and colleagues (2005) found differences in similar frontoparietal regions, although considerably weaker. These differences, however, appeared only at the end of their 10-s preparatory period, throughout which the task instruction cue (colored fixation point) remained visible. The findings of Curtis and D'Esposito (2003) and Ford et al. (2005)

suggest that subjects may postpone task-specific preparation until the end of a fixed-length instruction interval. Future studies making a direct comparison of short and long instruction intervals could directly test this prediction.

Preparatory differences in DLPFC were highly asymmetric in our study, with only left DLPFC exhibiting a large, statistically significant cluster of voxels with higher preparatory activation for antisaccade trials. The antisaccade fMRI literature is somewhat inconsistent on DLPFC and hemispheric asymmetry. Desouza et al. (2003) found greater preparatory activity for antisaccades than for prosaccades in right DLPFC only. Ford et al. (2005) found a similar result but in left rather than right DLPFC. Ford et al. also found greater preparatory activity for correct antisaccades than for error antisaccades in right DLPFC only. Curtis and D'Esposito (2003) and Connolly et al. (2002) did not investigate DLPFC for technical reasons. Given these inconsistencies, it would be premature to make strong statements on hemispheric asymmetry with regard to DLPFC's role in antisaccade performance.

Task preparation versus response generation

Response-related activations were greater for antisaccades than for prosaccades in several of the cortical saccade regions that exhibited preparatory differences (see above), consistent with our previous rapid event-related results (Brown et al. 2006). As we suggested in that study, greater response-related activation for antisaccades than for prosaccades could arise from a variety of processes, including the visuospatial remapping required to perform the antisaccade task and a more voluntary motor command with increased attention on antisaccade trials. Interestingly, an event-related fMRI study that used long instruction periods of $\geq$6 s did not find any differences between pro- and antisaccades during the response period (Desouza et al. 2003). We hypothesize that the long instruction periods in that study made the prosaccade task less automatic and therefore diminished activation differences.

Although the areas that make up the "classical" cortical saccade network, i.e., FEF, SEF, and IPS, showed differences during the preparatory period and during the response period, the ACC and the DLPFC did not show any differences in their response-related activation between prosaccades and antisaccades. This suggests that these two classical "control" areas are involved in the preparatory set for an antisaccade but not in the generation of the actual response. This hypothesis is also supported by studies in human subjects who suffered brain damage. Lesions of the dorsolateral prefrontal cortex in humans lead to increased error rates in the antisaccade task, but they do not impair the ability to generate an antisaccade or prosaccade (Guitton et al. 1985; Pierrot-Deseilligny et al. 1991, 2002, 2003; Ploner et al. 2005). The same finding has been reported for lesions of the anterior cingulate cortex (Gaymard et al. 1998). In contrast, damage to FEF (Gaymard et al. 1999) and IPS (Pierrot-Deseilligny et al. 1991) does not increase error rates in the antisaccade task, but it decreases the gain and increases the reaction times of contralateral saccades.

Processes related to frontoparietal activation

The frontoparietal activation evoked by the onset of an instruction stimulus will certainly reflect a variety of different processes. Indeed, a similar activation pattern is produced by increases in task difficulty in a multitude of cognitive tasks (Desimone and Duncan 1995; Miller and Cohen 2001). Compared with the performance of a prosaccade, the correct performance of an antisaccade requires at least two additional processes. The subject must first suppress the automatic response to look toward the flashed visual stimulus and then invert the stimulus location into a voluntary motor command to look away from the stimulus. Single-neuron recordings in monkeys have provided evidence that the brain accomplishes the first process by reducing the level of preparatory activity in the saccadic eye movement system before the stimulus appears (Munoz and Everling 2004). Saccade-related neurons in the superior colliculus (SC) and FEF have a lower level of activity during the preparatory period on antisaccade trials than that on prosaccade trials. Fixation-related neurons in these areas show the reverse pattern of activity. Higher levels of preparatory activity for antisaccades than for prosaccades have been found in the SEF (Amador et al. 2004). A large percentage of neurons in the DLPFC also exhibit differential preparatory activity between pro- and antisaccade trials (Everling and DeSouza 2005). The DLPFC is connected to a large number of cortical and subcortical areas, and Miller and Cohen (2001) have proposed that it provides bias signals for task-relevant processing to other areas. Indeed, it has recently been demonstrated that neurons in the DLPFC that project directly to the SC exhibit higher activity during the preparatory period on antisaccade trials than on prosaccade trials (Johnston and Everling 2006a). This finding is consistent with the idea that the DLPFC provides saccade-suppression signals to the SC (Gaymard et al. 2003). Many neurons in the ACC also exhibit different levels of preparatory activity between prosaccade and antisaccade trials, and this difference actually appears earlier than those in the DLPFC following a task switch (Johnston et al. 2007). Johnston and colleagues (2007) therefore suggested that the ACC also provides preparatory bias signals to other brain areas. These areas include both the SC (Leichnetz et al. 1981) and FEF (Wang et al. 2004). Together these data suggest that the frontal activation reflects at least in part this presetting of the saccade circuitry for the antisaccade task.

It is not yet known whether neurons in the lateral intraparietal (LIP) area, the putative monkey homologue of the human IPS, also exhibit task-related differences in prestimulus excitation. Gottlieb and Goldberg (1999) recorded single-unit activity in area LIP while monkeys performed prosaccade and antisaccade trials. Similar to our paradigm, monkeys were instructed at the onset of each trial by the color of the central fixation point to generate either a prosaccade or antisaccade on stimulus presentation. However, half of the trials were randomly interleaved memory-guided prosaccade and antisaccade trials, in which the animals had initially to suppress a saccade. Therefore monkeys had to suppress a saccade also on 50% of the prosaccade trials. Although Gottlieb and Goldberg (1999) did not compare preparatory activity between pro- and antisaccade trials in their study, it would be surprising to find any differences in this particular design because the animals likely adopted a strategy in which they prepared to initially suppress a saccade on both antisaccade and prosaccade trials. The same argument applies to another study that used only memory-

guided prosaccade and antisaccade trials (Zhang and Barash 2000).

Although Gottlieb and Goldberg (1999) did not report any differences in preparatory activity between pro- and antisaccades, they observed a modest, but significant, increase in stimulus-related activity for antisaccades compared with prosaccades in the population of LIP neurons. This higher activity for antisaccades is likely critical for task performance because LIP neurons showed a reduced stimulus-related response on error antisaccade trials when monkeys looked toward the stimulus. Moreover, a small percentage of LIP neurons (12%) encoded reliable saccade direction signals. The higher stimulus-related activity of LIP neurons for antisaccades could be the basis of the enhanced BOLD activation that we found for antisaccade trials compared with prosaccade trials during the response period.

The parietal cortex has also been implicated in the process of vector inversion required for antisaccades by single-unit recordings in monkeys (Zhang and Barash 2000, 2004), human ERP (Everling et al. 1998), and human fMRI studies (Medendorp et al. 2005). The vector inversion, however, can start only once the peripheral stimulus has been presented. Although the parietal activation might reflect the preparation of neurons in these areas for this process, we would regard this explanation as unlikely.

Frontoparietal cortex and visuospatial attention

Curtis and colleagues (2005) interpreted the activation in FEF and IPS on catch trials as evidence for a role of these areas in the covert direction of attention to the space where the targets were expected to appear. This interpretation is in line with many experiments that have demonstrated that reorientation of attention is a core function of frontoparietal regions (Corbetta et al. 1998, 2000; Posner and Petersen 1990). The shift of attention to peripheral locations certainly contributes to the frontoparietal activation that we observed on half trials. Such shifts of attention, however, should occur on both prosaccade and antisaccade trials because subjects have to localize the stimulus in both tasks.

Hon et al. (2006) demonstrated that attended stimulus changes, even when they require no behavioral responses, are sufficient to evoke frontoparietal activation. The authors interpreted this finding as evidence that these regions are activated by the simple updating of attended information. According to their model, the change of color of the attended central fixation point might have been sufficient to evoke frontoparietal activation in our paradigm. However, this process cannot account for the higher activation for antisaccades compared with prosaccades that we found in frontoparietal regions in this study.

Retinotopy

Although not shown here, we did not find differences in activation between contralateral and ipsilateral saccades. A contralateral bias has recently been reported for the IPS and FEF in human fMRI studies (Curtis and D'Esposito 2006; Medendorp et al. 2005; Schluppeck et al. 2006), but this bias originated during delay periods when subjects prepared to generate a saccade toward a previously cued location. Sereno et al. (2001) and Kastner et al. (2007) also found contralateral activation biases in IPS and FEF, respectively, using memory-guided saccade tasks, but they did not separate activation evoked by visual stimulus processing, working memory, and saccade generation. All of these could have contributed to the contralateral biases observed. To our knowledge, no fMRI study that did not contain a spatial working memory/saccade preparation component has reported a contralateral saccade activation bias in humans. This might be surprising given the strong contralateral bias in cortical neural activity found in monkey electrophysiology studies, especially in the FEF (Bruce and Goldberg 1985; Schall 1997). This difference might be related to the poor temporal resolution of fMRI, which makes it impossible to distinguish between activation caused by the saccade response and activation evoked by the subsequent return saccade. It is also known that the activity of FEF neurons in monkeys is suppressed before saccade onset if the saccade is directed outside of their response fields (Everling and Munoz 2000; Schall et al. 1995; Seidemann et al. 2002). Thus the metabolic activity associated with the suppression of large populations of neurons in the ipsilateral and contralateral FEF might prevent the detection of a contralateral saccade bias with fMRI.

In conclusion, we suggest that higher activation on antisaccade trials in the frontoparietal network reflects mainly the presetting of the oculomotor circuitry for the antisaccade task. This presetting ultimately requires a reduction in preparatory activity in the superior colliculus before stimulus presentation so that the process initiated by the incoming visual signal does not reach the saccade threshold before the vector inversion process for the voluntary antisaccade is completed (Munoz and Everling 2004). We propose that the DLPFC and ACC, the only areas that were more active for antisaccades than prosaccades during the preparatory period but not during the response period, bias activation in FEF, SEF, IPS, and SC before stimulus onset.

ACKNOWLEDGMENTS

We thank K. Ford, K. Johnston, J. Phillips, and S. Wegener for helpful comments on an earlier version of the manuscript. We also thank J. Gati and J. Williams for help in data acquisition.

GRANTS

This work was supported by the Canadian Institutes of Health Research.

REFERENCES

Amador N, Schlag-Rey M, Schlag J. Primate antisaccade. II. Supplementary eye field neuronal activity predicts correct performance. *J Neurophysiol* 91: 1672–1689, 2004.

Bandettini PA, Jesmanowicz A, Wong EC, Hyde JS. Processing strategies for time-course data sets in functional MRI of the human brain. *Magn Reson Med* 30: 161–173, 1993.

Barberi EA, Gati JS, Rutt BK, Menon RS. A transmit-only/receive-only (TORO) RF system for high-field MRI/MRS applications. *Magn Reson Med* 43: 284–289, 2000.

Bell AH, Everling S, Munoz DP. Influence of stimulus eccentricity and direction on characteristics of pro- and antisaccades in non-human primates. *J Neurophysiol* 84: 2595–2604, 2000.

Boynton GM, Engel SA, Glover GH, Heeger DJ. Linear systems analysis of functional magnetic resonance imaging in human V1. *J Neurosci* 16: 4207–4221, 1996.

Brown MR, Goltz HC, Vilis T, Ford KA, Everling S. Inhibition and generation of saccades: rapid event-related fMRI of prosaccades, antisaccades, and nogo trials. *Neuroimage* 33: 644–659, 2006.

Bruce CJ, Goldberg ME. Primate frontal eye fields. I. Single neurons discharging before saccades. *J Neurophysiol* 53: 603–635, 1985.

Bullmore E, Long C, Suckling J, Fadili J, Calvert G, Zelaya F, Carpenter TA, Brammer M. Colored noise and computational inference in neurophysiological (fMRI) time series analysis: resampling methods in time and wavelet domains. *Hum Brain Mapp* 12: 61–78, 2001.

Cabeza R, Nyberg L. Imaging cognition II: an empirical review of 275 PET and fMRI studies. *J Cogn Neurosci* 12: 1–47, 2000.

Connolly JD, Goodale MA, Menon RS, Munoz DP. Human fMRI evidence for the neural correlates of preparatory set. *Nat Neurosci* 5: 1345–1352, 2002.

Corbetta M, Akbudak E, Conturo TE, Snyder AZ, Ollinger JM, Drury HA, Linenweber MR, Petersen SE, Raichle ME, Van Essen DC, Shulman GL. A common network of functional areas for attention and eye movements. *Neuron* 21: 761–773, 1998.

Corbetta M, Kincade JM, Ollinger JM, McAvoy MP, Shulman GL. Voluntary orienting is dissociated from target detection in human posterior parietal cortex. *Nat Neurosci* 3: 292–297, 2000.

Curtis CE, Cole MW, Rao VY, D'Esposito M. Canceling planned action: an fMRI study of countermanding saccades. *Cereb Cortex* 15: 1281–1289, 2005.

Curtis CE, D'Esposito M. Success and failure suppressing reflexive behavior. *J Cogn Neurosci* 15: 409–418, 2003.

Curtis CE, D'Esposito M. Selection and maintenance of saccade goals in the human frontal eye fields. *J Neurophysiol* 95: 3923–3927, 2006.

Dale AM. Optimal experimental design for event-related fMRI. *Hum Brain Mapp* 8: 109–114, 1999.

Desimone R, Duncan J. Neural mechanisms of selective visual attention. *Annu Rev Neurosci* 18: 193–222, 1995.

Desouza JF, Menon RS, Everling S. Preparatory set associated with pro-saccades and anti-saccades in humans investigated with event-related fMRI. *J Neurophysiol* 89: 1016–1023, 2003.

Dorris MC, Paré M, Munoz DP. Neuronal activity in monkey superior colliculus related to the initiation of saccadic eye movements. *J Neurosci* 17: 8566–8579, 1997.

Duncan J, Owen AM. Common regions of the human frontal lobe recruited by diverse cognitive demands. *Trends Neurosci* 23: 475–483, 2000.

Engel SA, Glover GH, Wandell BA. Retinotopic organization in human visual cortex and the spatial precision of functional MRI. *Cereb Cortex* 7: 181–192, 1997.

Evarts EV, Shinoda Y, Wise SP. *Neurophysiological Approaches to Higher Brain Function*. New York: Wiley, 1984.

Everling S, DeSouza JF. Rule-dependent activity for prosaccades and antisaccades in the primate prefrontal cortex. *J Cogn Neurosci* 17: 1483–1496, 2005.

Everling S, Dorris MC, Klein RM, Munoz DP. Role of primate superior colliculus in preparation and execution of anti-saccades and pro-saccades. *J Neurosci* 19: 2740–2754, 1999.

Everling S, Fischer B. The antisaccade: a review of basic research and clinical studies. *Neuropsychologia* 36: 885–899, 1998.

Everling S, Krappmann P, Flohr H. Cortical potentials preceding pro- and antisaccades in man. *Electroencephalogr Clin Neurophysiol* 102: 356–362, 1997.

Everling S, Munoz DP. Neuronal correlates for preparatory set associated with pro-saccades and anti-saccades in the primate frontal eye field. *J Neurosci* 20: 387–400, 2000.

Everling S, Spantekow A, Krappmann P, Flohr H. Event-related potentials associated with correct and incorrect responses in a cued antisaccade task. *Exp Brain Res* 118: 27–34, 1998.

Fischer B, Weber H. Characteristics of "anti" saccades in man. *Exp Brain Res* 89: 415–424, 1992.

Fischer B, Weber H. Effects of stimulus conditions on the performance of antisaccades in man. *Exp Brain Res* 116: 191–200, 1997.

Forbes K, Klein RM. The magnitude of the fixation offset effect with endogenously and exogenously controlled saccades. *J Cogn Neurosci* 8: 344–352, 1996.

Ford KA, Goltz HC, Brown MR, Everling S. Neural processes associated with antisaccade task performance investigated with event-related fMRI. *J Neurophysiol* 94: 429–440, 2005.

Gaymard B, Francois C, Ploner CJ, Condy C, Rivaud-Pechoux S. A direct prefrontotectal tract against distractibility in the human brain. *Ann Neurol* 53: 542–545, 2003.

Gaymard B, Ploner CJ, Rivaud-Pechoux S, Pierrot-Deseilligny C. The frontal eye field is involved in spatial short-term memory but not in reflexive saccade inhibition. *Exp Brain Res* 129: 288–301, 1999.

Gaymard B, Rivaud S, Cassarini JF, Dubard T, Rancurel G, Agid Y, Pierrot-Deseilligny C. Effects of anterior cingulate cortex lesions on ocular saccades in humans. *Exp Brain Res* 120: 173–183, 1998.

Gottlieb J, Goldberg ME. Activity of neurons in the lateral intraparietal area of the monkey during an antisaccade task. *Nat Neurosci* 2: 906–912, 1999.

Guitton D, Buchtel HA, Douglas RM. Frontal lobe lesions in man cause difficulties in suppressing reflexive glances and in generating goal-directed saccades. *Exp Brain Res* 58: 455–472, 1985.

Hallett PE. Primary and secondary saccades to goals defined by instructions. *Vision Res* 18: 1279–1296, 1978.

Hallett PE, Adams BD. The predictability of saccadic latency in a novel voluntary oculomotor task. *Vision Res* 20: 329–339, 1980.

Hebb DO. *Textbook of Physiology*. Philadelphia, PA: Saunders, 1972, p. 77.

Hon N, Epstein RA, Owen AM, Duncan J. Frontoparietal activity with minimal decision and control. *J Neurosci* 26: 9805–9809, 2006.

Johnston K, Everling S. Monkey dorsolateral prefrontal cortex sends task-selective signals directly to the superior colliculus. *J Neurosci* 26: 12471–12478, 2006a.

Johnston K, Everling S. Neural activity in monkey prefrontal cortex is modulated by task context and behavioral instruction during delayed-match-to-sample and conditional prosaccade-antisaccade tasks. *J Cogn Neurosci* 18: 749–765, 2006b.

Johnston K, Levin HM, Koval MJ, Everling S. Top-down control-signal dynamics in anterior cingulate and prefrontal cortex neurons following task switching. *Neuron* 53: 453–462, 2007.

Kastner S, Desimone K, Konen CS, Szczepanski SM, Weiner KS, Schneider KA. Topographic maps in human frontal cortex revealed in memory-guided saccade and spatial working-memory tasks. *J Neurophysiol* 97: 3494–3507, 2007.

Klassen LM, Menon RS. Robust automated shimming technique using arbitrary mapping acquisition parameters (RASTAMAP). *Magn Reson Med* 51: 881–887, 2004.

Klein C, Heinks T, Andresen B, Berg P, Moritz S. Impaired modulation of the saccadic contingent negative variation preceding antisaccades in schizophrenia. *Biol Psychiatry* 47: 978–990, 2000.

Leichnetz GR, Spencer RF, Hardy SG, Astruc J. The prefrontal corticotectal projection in the monkey; an anterograde and retrograde horseradish peroxidase study. *Neuroscience* 6: 1023–1041, 1981.

Medendorp WP, Goltz HC, Vilis T. Remapping the remembered target location for anti-saccades in human posterior parietal cortex. *J Neurophysiol* 94: 734–740, 2005.

Miller EK, Cohen JD. An integrative theory of prefrontal cortex function. *Annu Rev Neurosci* 24: 167–202, 2001.

Munoz DP, Everling S. Look away: the anti-saccade task and the voluntary control of eye movement. *Nat Rev Neurosci* 5: 218–228, 2004.

Ollinger JM, Corbetta M, Shulman GL. Separating processes within a trial in event-related functional MRI. *Neuroimage* 13: 218–229, 2001a.

Ollinger JM, Shulman GL, Corbetta M. Separating processes within a trial in event-related functional MRI. *Neuroimage* 13: 210–217, 2001b.

Pierrot-Deseilligny C, Muri RM, Ploner CJ, Gaymard B, Demeret S, Rivaud-Pechoux S. Decisional role of the dorsolateral prefrontal cortex in ocular motor behaviour. *Brain* 126: 1460–1473, 2003.

Pierrot-Deseilligny C, Ploner CJ, Muri RM, Gaymard B, Rivaud-Pechoux S. Effects of cortical lesions on saccadic: eye movements in humans. *Ann NY Acad Sci* 956: 216–229, 2002.

Pierrot-Deseilligny C, Rivaud S, Gaymard B, Agid Y. Cortical control of reflexive visually-guided saccades. *Brain* 114: 1473–1485, 1991.

Ploner CJ, Gaymard BM, Rivaud-Pechoux S, Pierrot-Deseilligny C. The prefrontal substrate of reflexive saccade inhibition in humans. *Biol Psychiatry* 57: 1159–1165, 2005.

Posner MI, Petersen SE. The attention system of the human brain. *Annu Rev Neurosci* 13: 25–42, 1990.

Schall JD. Visuomotor areas of the frontal lobe. *Cereb Cortex* 12: 527–638, 1997.

Schall JD, Hanes DP, Thompson KG, King DJ. Saccade target selection in frontal eye field of macaque. I. Visual and premovement activation. *J Neurosci* 15: 6905–6918, 1995.

Schluppeck D, Curtis CE, Glimcher PW, Heeger DJ. Sustained activity in topographic areas of human posterior parietal cortex during memory-guided saccades. *J Neurosci* 26: 5098–5108, 2006.

Seidemann E, Arieli A, Grinvald A, Slovin H. Dynamics of depolarization and hyperpolarization in the frontal cortex and saccade goal. *Science* 295: 862–865, 2002.

Serences JT. A comparison of methods for characterizing the event-related BOLD timeseries in rapid fMRI. *Neuroimage* 21: 1690–1700, 2004.

Sereno MI, Pitzalis S, Martinez A. Mapping of contralateral space in retinotopic coordinates by a parietal cortical area in humans. *Science* 294: 1350–1354, 2001.

Wang Y, Matsuzaka Y, Shima K, Tanji J. Cingulate cortical cells projecting to monkey frontal eye field and primary motor cortex. *Neuroreport* 15: 1559–1563, 2004.

Worsley KJ, Liao CH, Aston J, Petre V, Duncan GH, Morales F, Evans AC. A general statistical analysis for fMRI data. *Neuroimage* 15: 1–15, 2002.

Zhang M, Barash S. Neuronal switching of sensorimotor transformations for antisaccades. *Nature* 408: 971–975, 2000.

Zhang M, Barash S. Persistent LIP activity in memory antisaccades: working memory for a sensorimotor transformation. *J Neurophysiol* 91: 1424–1441, 2004.